

Copper Transport and Accumulation in Spruce Stems (*Picea abies* (L.) Karsten) Revealed by Laser-Induced Breakdown Spectroscopy

Lucie Krajcarova¹, Karel Novotny^{1,2}, Petr Babula^{2,3}, Ivo Provaznik⁴, Petra Kucerova^{1,2}, Vojtech Adam^{2,5}, Madhavi Z. Martin⁶, Rene Kizek^{2,5}, and Jozef Kaiser^{2,7,*}

¹ Department of Chemistry, Faculty of Science, Masaryk University, Kotlarska 2, CZ-611 37 Brno, Czech Republic, European Union

² Central European Institute of Technology, Brno University of Technology, Technicka 3058/10, CZ-616 00 Brno, Czech Republic, European Union

³ Department of Natural Drugs, Faculty of Pharmacy, University of Veterinary and Pharmaceutical Sciences, Palackeho 1-3, CZ-612 42 Brno, Czech Republic, European Union

⁴ Department of Biomedical Engineering, Faculty of Electrical Engineering and Communication, Kolejní 2906/4, 612 00, Brno, Czech Republic, European Union

⁵ Department of Chemistry and Biochemistry, Faculty of Agronomy, Mendel University in Brno, Zemedelska 1, CZ-613 00 Brno, Czech Republic, European Union

⁶ BioSciences Division, Oak Ridge National Laboratory, Oak Ridge, TN 37831, USA

⁷ Institute of Physical Engineering, Faculty of Mechanical Engineering, Brno University of Technology, Technická 2896/2, 616 69 Brno, Czech Republic, European Union

*E-mail: kaiser@fme.vutbr.cz

Received: 20 October 2012 / Accepted: 4 December 2012 / Published: 1 April 2013

Laser-Induced Breakdown Spectroscopy (LIBS) in double pulse configuration (DP LIBS) was used for scanning elemental spatial distribution in annual terminal stems of spruce (*Picea abies* (L.) Karsten). Cross sections of stems cultivated in Cu²⁺ solution of different concentrations were prepared and analyzed by DP LIBS. Raster scanning with 150 μm spatial resolution was set and 2D (2-dimensional) maps of Cu and Ca distribution were created on the basis of the data obtained. Stem parts originating in the vicinity of the implementation of the cross sections were mineralized and subsequently Cu and Ca contents were analyzed by inductively coupled plasma mass spectrometry (ICP-MS). The results provide quantitative information about overall concentration of the elements in places, where LIBS measurements were performed. The fluorescence pictures were created to compare LIBS distribution maps and the fluorescence intensity (or the increase in autofluorescence) was used for the comparison of ICP-MS quantitative results. Results from these three methods can be utilized for quantitative measurements of copper ions transport in different plant compartments in dependence on the concentration of cultivation medium and/or the time of cultivation.

Keywords: Electrochemical Detection; Double-pulse LIBS; Fluorescence Microscopy; Elemental Distribution; Mass Spectrometry

1. INTRODUCTION

Plants absorb not only nutrient elements from the environment, but also some nonessential and essential trace elements including metals. Some of the metals (*e.g.* Fe, Mn, Zn, Cu, Ni, Mo) are essential microelements for plants, others as Ag, Au and Co are considered as nonessential, yet they are known to stimulate plant growth. Finally, plants also absorb metals, which are toxic even at low concentration (*e.g.* Cd, Hg, As, Pb, Cr) with no known biological function [1]. Transition metals are very important for all organisms due to their capability to receive and provide electrons (redox reactions), but in case of their excessive intake they could become toxic due to the production of reactive oxygen forms (oxidative stress). Plants use a few regulation mechanisms to maintain metal homeostasis. They adjust the cellular concentrations of metals in dependence on external conditions by means of the regulation of metal intake, transport, storage and precipitation [2]. Here we present the results of the study on intake, distribution and accumulation of copper in annual terminal stems of spruce. Copper is a redox-active transition metal associated with many physiological processes in plants. It is one of the essential trace elements, which are important in many biochemical processes of prokaryotes and eukaryotes. As a structural element of the regulation proteins it is involved in the electron transport mechanisms during the photosynthesis and also in the mitochondrial respiration, in oxidative stress response, in the cell wall metabolism and hormonal signalization. Copper ions are cofactors of many enzymes, *e.g.* Cu/Zn superoxide dismutase (Cu/Zn SOD), cytochrome c oxidase, amino oxidase, plastocyanin and polyphenol oxidase. Copper is also important in processes on the cellular level, *e.g.* signalization of transcription, the oxidative phosphorylation and iron mobilization [3]. In case of copper deficiency specific symptoms occur on plants such as damage on the reproductive organs and young leaves. On the other hand, copper redox-activity can lead to production of high toxic hydroxyl radicals, which can cause damage of the DNA, proteins, lipids and other biomolecules [4]. Thus copper can be extremely toxic in the excessive amount and it can cause specific excess symptoms on plant, *e.g.* chlorosis, necrosis, stunting, leaves discoloration and inhibition of root growth [5-7]. Numerous studies have greatly enhanced the present knowledge of Cu absorption mechanisms, but these are still far from being understood. It may be stated that, however, there is increasing evidence of the active absorption of copper and passive absorption is likely to occur, especially in the toxic concentration range of this metal in solutions [8]. The plants exhibiting tree characteristics were chosen for our experiment. Trees have promising potential *e.g.* in the process of phytoremediation. This technique uses plants for in situ risk reduction and/or removal of contaminants from polluted soil, water, sediments and air. The main aspects that determine plants suitability for phytoremediation are their sufficient accumulation, resistance and massive shoot and aerial biomass production. The utilization of trees for phytoremediation is convenient in contaminated areas especially for economic reasons or when there is no time pressure on the reuse of the land [9]. The tree vegetation cover decreases the risk of air and water erosion via physical stabilization of soil with the root system. The leaf shed provides indispensable amount of organic matter for surface layers of soils and thus supports nutrition cycle, soil aggregation and soil water capacity. Huge amount of water

engaged in tree transpiration process reduces the down flow of water through the soil and thus holds down the amount of heavy metal in ground and surface water [9]. There have been papers published concerning tree species which naturally colonize the investigated sites, for example, *Betula pendula*, *Alnus glutinosa*, *Salix viminalis*, *Pinus contorta*, etc. [10-12]. For the purpose of our experiment, *Picea abies* (L.) Karsten was used as there are only few papers devoted to this topic and also because this tree species together with other trees (*Betula pendula*, *Pinus sylvestris*) is planted in the recultivation areas (e.g. Smolník in the Slovak Republic).

The most routinely used techniques for the analysis of plant samples are atomic absorption spectrometry (AAS), inductively coupled plasma atomic emission spectrometry (ICP-AES), neutron activation analysis (NAA), X-ray fluorescence analysis (XRF), ICP mass spectrometry (ICP-MS) or ICP optical emission spectrometry (ICP-OES). The acquired pieces of information are applicable e.g. in the study of molecular biology, plant physiology and environment, in agriculture or in food quality monitoring. Nevertheless, most of these methods require conversion of solid samples into solution or other sample treatment and thus the information about distribution of elements within samples is lost. That is why the methods allowing the mapping of spatial elemental distribution are developed. For plant samples time of flight secondary ion mass spectrometry (TOF-SIMS) [13], laser ablation inductively coupled plasma mass spectrometry (LA-ICP-MS) [14,15], laser-induced breakdown spectrometry (LIBS) [16,17], or matrix assisted laser desorption ionization mass spectrometry (MALDI-MS) are used [18].

LIBS is a convenient analytical technique for plant samples due to minimal sample preparation requirements and the possibility of multielemental, *real-time* and *in-situ* measurements [19]. In previous works LIBS was successfully used for monitoring the plant elemental composition. [20] used LIBS for direct determination of selected elements in powdered plant leaves. They used NIST standard reference materials as test samples and investigated the reliability of LIBS measurements. [21] used femtosecond LIBS to determine the spatial distribution of Fe within the leaf of maize and *Cornus stolonifera*. [22] determined Cd and Pb in leaves and roots of cultivated sunflower (*Helianthus annuus* L.) by X-ray microradiography and observed femtosecond LIBS spectra which gave comparable results. In another study [23] they cultivated sunflower in Pb EDTA solutions with different concentrations and subsequently mapped Pb and Mg in with LIBS and LA-ICP-MS (200 μm resolution). They compared results with AAS and TLC outcomes. [16] mapped the central leaf vein and surrounding parts of cultivated sunflower (*Helianthus annuus* L.) by nanosecond LIBS and observed increased Pb intensity in vein. In their other work [24] they mapped also Ag and Cu in sunflower leaves and the results were compared with LA-ICP-MS mapping. In the case of both methods they observed increased amount of Ag in the vein structures. In the work of Juvé *et al.* nanosecond UV LIBS system was applied to analyze trace elements in fresh vegetables (root of potato and carrot, stem of celery and fruit of aubergine). Space-resolved analysis was performed taking advantage of the high spatial resolution of the technique [25]. In the work of [26] LIBS method was evaluated for the determination of macronutrients (P, K, Ca, Mg) in pellets of vegetal reference materials. Certified reference materials as well as reference materials were used for analytical calibrations of P, K, Ca, and Mg. Most of the results were in reasonable agreement with those obtained by ICP OES after wet acid decomposition. In their other work [27] they used LIBS for determination

of micronutrients (B, Cu, Fe, Mn and Zn) in pellets of plant materials, using NIST, BCR and GBW biological certified reference materials for analytical calibration. [28] demonstrated in their study that LIBS combined with multivariate analysis can be employed to analyze the chemical composition of annual tree growth rings, which can be subsequently correlated to environmental parameters such as changes in climate, forest fires, and disturbances involving human activity. In another study [29] LIBS was used to determine the impact of endophyte infection on elemental composition of tall fescue (*Festuca arundinacea* Schreb.). LIBS was established as the method useful for detection of Fe, Mn, Mg, Pb, Ca, Zn and Cd, however, the determination of endophyte impact was not incontrovertibly observed.

Large number of works has recently been published dealing with the mechanisms of the metal intake, transport, tolerance, mobilization and accumulation in plants [1,5-7,30-32]. In most of them the mechanisms on cellular level and biochemical processes are discussed. Moreover, there are also many studies about the transport from soils to root and shoot systems, but only on the soil-root, root-stem, root-leaves or stem-grains levels. The information about the elements distribution and remobilization in terms of plant tissues is poorly available. Here we report on the spatial copper and calcium distribution in plant tissues on the cross sections of plant stem.

2. EXPERIMENTAL PART

2.1 Plant material

For this experiment, 15 cm long annual terminal stems of spruce (*Picea abies*) (L.) Karsten were collected. These stems were placed into beakers filled till 5 cm with CuCl_2 (Sigma Aldrich, USA) solution with concentration of 1; 5; 10 and 50 mmol.l^{-1} and into a beaker with distilled water as the control sample. All beakers with stems were put into plant chamber and cultivated under following conditions: $25 \pm 1^\circ \text{C}$, relative air humidity $80 \pm 5\%$ and illuminance 10 000 lux.

2.2 Plant material for microscopy

After 2 hours one stem from each beaker was taken out and immediately thin cross sections (1-2 mm) in five places on stems distant 2 cm from each other were prepared. Locations on stems are marked A-E. While A is situated in the apex of the stem, E is above the surface of the solution. From each location there were two slices taken in total, one for LIBS measurement and the other for fluorescence microscopy imaging (Fig. 1). The same procedure was realized in strictly defined time intervals of 4; 8; 16 and 24 hours of cultivation. Slices were fixed onto slides with glycerol jelly as mounting medium. The slides were stored in freezer during experiment duration.

2.3 Plant material mineralisation

Moreover, small stem parts (about 1 mm long) originated in the vicinity of the implementation of cross sections were collected. They were dried till constant weight (3 hours) in common laboratory drier (ECOCELL) heated up to 105°C . Weights of the dry mass were approximately 500 mg. Each

sample was mineralized with 4 ml conc. HNO₃ and 2 ml 30% H₂O₂ in microwave mineralizer. Resulting solutions were filled up with distilled water into 50 ml volumetric flask and analyzed with ICP-MS.

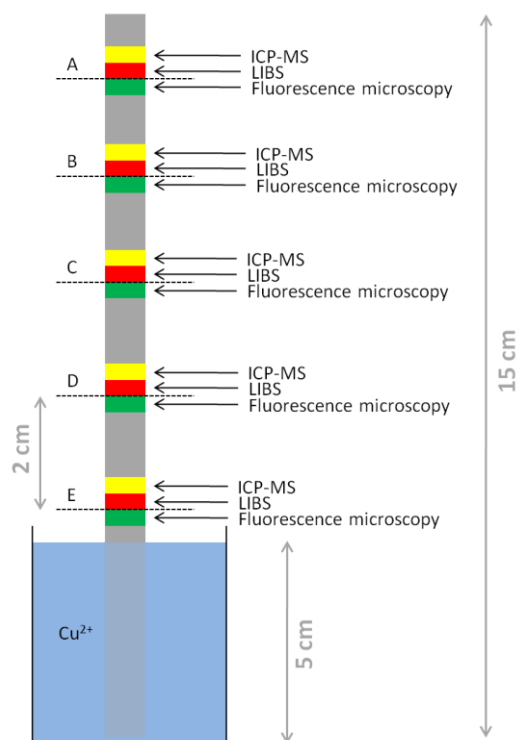


Figure 1. The scheme of experimental cultivation, condition and sample preparation.

2.4 LIBS experimental

For 2D mapping of elemental distribution the orthogonal re-heating double pulse LIBS configuration was used. The first laser which irradiated the sample surface was Nd:YAG laser operated at fourth harmonic frequency 266 nm (New Wave, UP-266 MACRO) with the energy of 10 mJ per pulse. The short wavelength of this laser provides the creation of small ablation crater in the sample, which was about 100 μm in these experiments. The laser system UP-266 MACRO was equipped with a sample holder with software-controlled movement in x , y direction and hand-controlled z direction movement. The slide with a sample was firmly fixed on the holder and measured in the air at atmospheric pressure. As the second, re-heating laser beam propagated parallel to the sample surface Quantel, Brilliant Nd:YAG laser at fundamental wavelength 1064 nm and energy 100 mJ per pulse was used. This laser was focused by 80 mm focal length glass lens to intersect the path of the first laser beam and finally to create a coincident spark about 0.5 mm above the sample surface. The volume of the emitting plasma increases under the effect of the second laser pulse resulting in signal enhancement. This phenomenon takes place due to more uniform absorption of the second laser pulse while its energy is distributed over larger volume. The limits of detection are lowered and signal-to-noise ratio is improved in comparison with the single pulse mode.

Both lasers were externally triggered by two delay generators (Stanford Research Systems, DG 645). The first generator initialized with the control pulse from the flash lamp of UP-266 MACRO laser module was used to trigger the flash lamp of the first laser (UP-266 MACRO) and the second laser (Quantel, Brilliant). The second generator was handled by Q-switch control pulse of UP-266 MACRO laser module and was utilized to trigger Q-switches of both lasers. The delay of opening the second laser's Q-switch after the first ones determines the inter-pulse delay. For our samples 500 ns optimal inter-pulse delay was established. The second generator was also used for ICCD detector triggering. The energy of the laser was measured with laser power/energy meter (Nova, Ophir). The plasma emission was collected and transported by means of 3 m long optical fiber into the monochromator (Jobin Yvon, TRIAX 320) (grating 2400 grooves. mm^{-1} , 50 μm entrance slit) and detected with the ICCD detector (Jobin Yvon, Horiba). The delay of the ICCD detector was 1 μs and the integration time was 10 μs . The spectral resolution of Jobin Yvon TRIAX with this grating was 0.028 nm. The ablation repetition rate was 1 Hz to ensure uploading all the data from the ICCD camera for each measured spot. The software of UP-266 MACRO allows the setting of all laser parameters and stage positioning and provides sample viewing. The software also offers variety of measuring modes such as spot ablation for depth profiling, line scanning for lateral analysis and also raster scanning for bulk and surface analysis. All the slices obtained from stems of *Picea abies* (L.) Karsten were measured by the described system set in raster scanning mode. Point distance 150 μm was set in both x and y directions. The emitted light after one laser shot was detected for each point (single-shot measurement, Fig. 2).

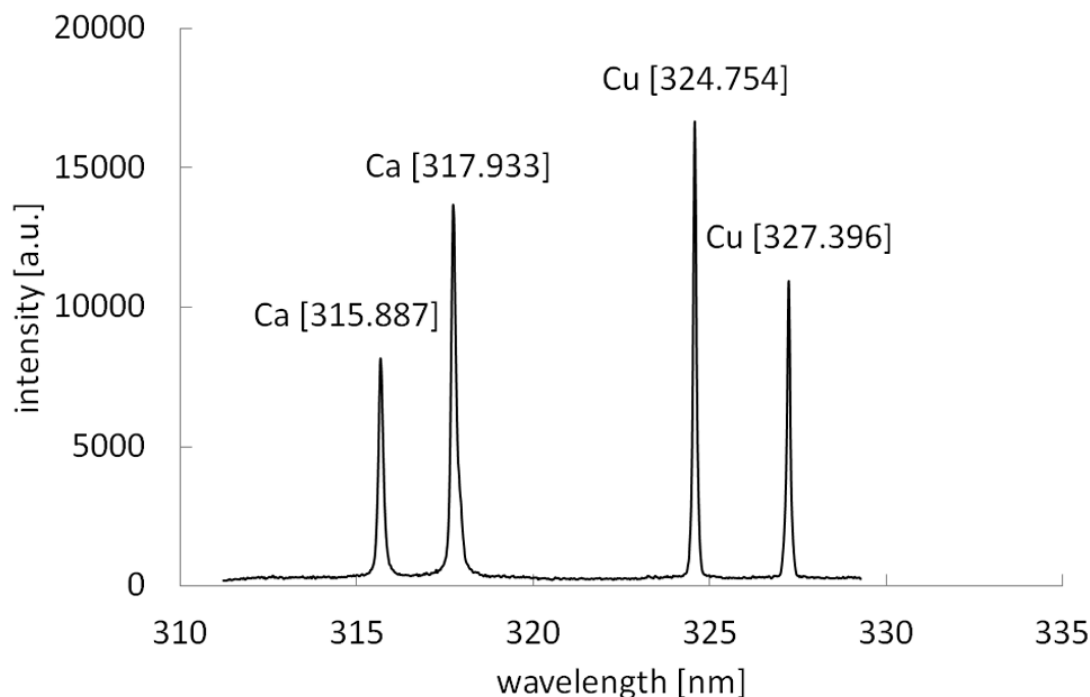


Figure 2. A typical LIBS spectrum with Ca(II) 317.933 nm and Cu(I) 324.754 nm lines used for creating the maps, other experimental condition see in chapter 2.2.

For the data analysis the lines at 324.754 nm Cu(I) and 317.933 nm Ca(II) were chosen. From each of the investigated spectral line the continuum background determined by the intensities of six data points on both line sides was subtracted by linear background fit method. There was no additional normalization to the background used. The resulting data were aligned according to raster points and 2D maps of Cu and Ca distribution on each stem slice were prepared.

2.5 ICP-MS experimental

The total content of Cu and Ca in dissolved samples was investigated with the ICP-MS spectrometer (Agilent, 7500ce) with quadrupole analyser (Agilent, Japan). Samples were nebulized into plasma via microconcentric nebulizer (Sono-Tek Corporation, MicroMist) with the uptake of 0.1 ml.min⁻¹. The distance from the load coil to the sample cone (sampling depth) was 8 mm. The power of RF coil was set at 1.45 W. Argon was used as the carrier gas with the flow of 0.90 l.min⁻¹. The main gas Ar of 15 l.min⁻¹ and makeup gas Ar of 0.19 l.min⁻¹ were used. The collision cell for isobar interferences elimination is a part of this instrumentation. The flow of both gases H and He used for collision was 2.5 ml.min⁻¹. The electron multiplier was used as a detector. The optimization procedure is detailed in Galiová et al. (2010). For the construction of Cu and Ca calibration curves the solutions from standard materials (Analytika, Astatol, Prague, CZ) were prepared. Each sample was measured three times and standard deviation was calculated automatically by ICP-MS software.

2.6 Electrochemical determination

For electrochemical detection of metal peak differential pulse voltammetry (DPV) and anodic stripping differential pulse voltammetry (ASVDPV) were applied. All measurements were performed in an electrochemical cell with the classic three electrode system, where the mercury electrode (SMDE) was a working electrode, reference electrode was an argent-chloride (Ag/AgCl/3M KCl) electrode and auxiliary electrode was a glassy carbon electrode. All measurements were performed in acetate buffer (pH 5.0) at temperature 25 °C. Samples were deoxygenated by argon (99.99%, 120 s). Measurements were carried out at an Autolab analyzer, in connection with VA-Stand 663, 800 Dosino, 846 Dosing Interface (all from Metrohm Autolab, Switzerland). To results evaluation the GPES software was used. The parameters of DPV determination were as follows: initial potential 0.15 V; end potential -1.3 V; deposition potential 0.15 V; duration 240 s; equilibration time 5 s; modulation time 0.06 s; time interval 0.2 s; potential step 0.002 V; modulation amplitude 0.025 V. The parameters of DPV stripping heavy metals determination were as follows: initial potential -1.3 V; end potential 0.15 V; deposition potential -1.3 V; duration 240 s; equilibration time 5 s; modulation time 0.06 s; time interval 0.2 s; potential step 0.002 V; modulation amplitude 0.025 V. Other experimental details see in papers [33-38].

2.7 Fluorescence microscopy

For the determination of autofluorescence of samples, fresh sections (30 µm) were directly observed using a fluorescence microscope Axioscop AX40 (Zeiss, Germany) equipped with wide-

broad UV excitation and a set of barrier filters (FITC, DAPI, Cy3 and Cy5). For the determination of copper (II) ions in plant tissue both light and fluorescence microscopies were used. Cupron (benzoinoxime) and diphenylcarbazide (both Sigma-Aldrich, USA) were utilized for rapid determination of Cu in plant tissue. For the purpose of more specific evaluation of Cu distribution, derivative of rhodanine (5-(4-dimethylaminobenzylidene)rhodanine) (Sigma-Aldrich, USA) was applied for fluorescence microscopy. The images were observed with fluorescence microscope Axioscop AX40 (Zeiss, Germany) equipped with wide-broad UV excitation and a set of barrier filters (FITC, DAPI, Cy3 and Cy5), the photos were acquired via camera ProgRes MF (Jenoptik, Germany). NIS elements software (Nikon, Japan) was employed for evaluation of changes in fluorescence/autofluorescence.

2.6 Mathematical treatment of data

Mathematical analysis of the data and their graphical interpretation was realized by software Matlab (version 7.11.). Results are expressed as mean \pm standard deviation (S.D.) unless noted otherwise (EXCEL®). The data was interpolated and maps were created using Matlab 7.13 (2011b) software.

3. RESULTS AND DISCUSSION

3.1 LIBS - analysis

Coordinated functions of uptake, buffering, translocation and storage processes are required to maintain essential metal concentrations in various tissues and compartments within the narrow physiological limits [39]. The distribution and accumulation patterns of trace elements vary considerably for each element and plant species [8]. The transport of ions within plant tissues and organs involves many processes: (1) movement in xylem, (2) movement in phloem, (3) storage, accumulation, and immobilization. As it was described above in detail, for the mapping of copper ions in plant tissues LIBS measurement was utilized. Typical maps can be seen in Fig. 3.

The previously discussed facts can explain that in the case of our samples the most significantly increased intensity signal of Cu was usually situated in areas of the primary and secondary xylem and phloem. Metals are translocated by membrane metal transporters and metal-binding proteins to their final destination. This process involves specific proteins (*e.g.* metallothioneins, metallochaperones or low molecular weight metal chelators) that must maintain fine balance between having enough essential metals available for metabolic functions while avoiding deficiency or toxicity [40-47]. Excess metals are stored in such location, where the metal can do the least harm to cellular processes. This involves storage in special cellular compartments such as vacuoles. Sequestration may also be realized in the apoplast, or in specialized cells such as epidermal cells and trichomes [3]. These all could be the reasons why the decreasing copper intensity in green and highly metabolic active tissues is observed, whereas in secondary dermal tissues the intensity is often increased.

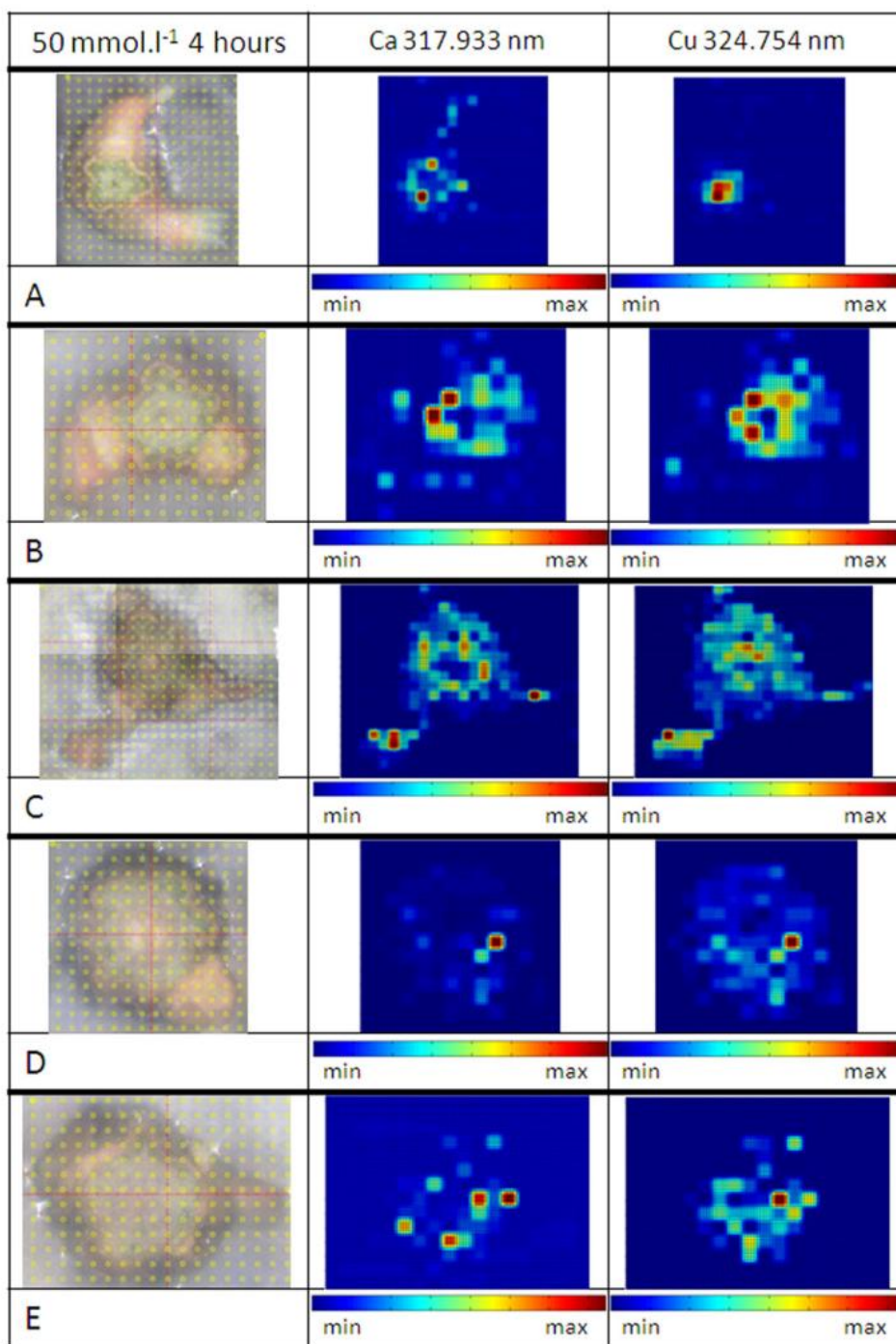


Figure 3. Series of the LIBS intensity maps showing the distribution of Ca (in the middle) and Cu (on the right side) on slices of stem of *Picea abies* (L.) Karsten. Other experimental conditions see in Experimental Section.

3.2 ICP-MS

The set of data concerning the overall concentrations of Cu and Ca nearby A-E positions in stems of *Picea abies* (L.) Karsten was obtained after different treatments via ICP-MS analysis (Tab.1).

Table 1. The amount of copper evaluated with ICP-MS and electrochemistry solution analysis (in mg.kg^{-1}). On the right side of the table the trend maps of acquired amounts are visualized.

		2 h	4 h	8 h	16 h	24 h	
0 (control)	A	5.23	7.12	7.61	6.99	8.25	
	B	6.15	6.63	5.21	8.22	6.80	
	C	7.93	5.53	8.32	7.07	16.47	
	D	6.40	5.21	9.46	10.77	5.57	
	E	3.37	4.99	4.58	4.05	14.97	
1 mmol.l^{-1}	A	3.33	3.70	4.84	5.82	4.04	
	B	1.06	1.23	3.04	3.08	2.60	
	C	3.05	4.78	4.43	6.70	11.52	
	D	5.20	5.94	13.40	120.09	29.57	
	E	877.22	385.58	2060.62	457.47	315.71	
5 mmol.l^{-1}	A	4.50	4.64	5.71	7.27	4.57	
	B	2.95	2.23	3.55	4.21	11.86	
	C	3.81	1.57	11.00	90.15	158.45	
	D	90.98	164.74	229.82	1271.80	481.07	
	E	656.93	1136.57	1535.83	882.78	2413.27	
10 mmol.l^{-1}	A	6.67	19.80	5.60	5.25	9.76	
	B	3.73	4.11	5.47	19.58	51.93	
	C	3.73	7.65	258.76	145.52	123.23	
	D	81.31	73.23	394.31	435.63	1587.68	
	E	1651.61	4014.80	1812.14	2260.70	1998.98	
50 mmol.l^{-1}	A	3.96	24.57	44.79	289.98	1007.81	
	B	3.31	143.29	572.16	805.51	693.15	
	C	84.24	584.91	634.43	770.88	4375.57	
	D	1086.74	1058.00	1120.56	525.08	3152.50	
	E	1595.63	3728.43	4537.30	5292.95	6872.05	

The Ca 44 isotope and Cu 63 isotope were detected. The limits of detection (LOD) were established from calibration curves. The LOD for Ca is $660 \mu\text{g.kg}^{-1}$ and for Cu $13 \mu\text{g.kg}^{-1}$. Throughout vegetation the average value of Cu is $5.1\text{-}30 \text{mg.kg}^{-1}$ [8]. Control samples in our measurement treated with water had Cu content of $3.4\text{-}16.5 \text{mg.kg}^{-1}$ (Tab.1). The value 3.4mg.kg^{-1} belongs among deficiency values that range within $2\text{-}5 \text{mg.kg}^{-1}$ in vegetation. This value was the very minimum in our control samples, all the other values were usually in the normal range (Tab. 1). An interesting fact is that Cu contents in A, B and C position are sometimes in deficiency range even after the treatment in CuCl_2 solution (e.g. 5mmol.l^{-1} after 4 hours of cultivation, see Tab. 1). Values $20\text{-}100 \text{mg.kg}^{-1}$ are considered as excessive, these values may be inside the phytotoxic level ranges (typically $60\text{-}125$

mg.kg⁻¹ as it was reported in Kabata-Pendias and Pendias [8]). In our experiment Cu amount is often much higher than the phytotoxic values, especially in E position that is very next to the solution surface. In order to avoid metal toxicity, all plants possess basal tolerance mechanisms, which appear to be involved primarily in avoiding the accumulation of toxic concentrations at sensitive sites within the cell. This prevents the damaging effects rather than developing the proteins that can resist the heavy metal effects. The potential cellular mechanisms involved in tolerance include those by:

- 1 reducing metal uptake through mycorrhiza action or extracellular exudates;
- 2 immobilizing excess of Cu in the root and thus excluding the metal from the shoot;
- 3 stimulating the efflux pumping metal at the plasma membrane;
- 4 chelation of metals by phytochelatins, metallothioneins, organic acids or heat shock proteins;
- 5 compartmentation of metals in the vacuole [6,48].

The treatment was applied only to stem cuttings with no roots in our experiment and thus some of these plant tolerance mechanisms were impossible to utilize. Probably from these reasons and moreover because the concentrations of CuCl₂ solution for sample cultivation were very high, the amounts of Cu in samples are much higher than normal values and often very high also in comparison to phytotoxic values. The critical free Cu concentration in the nutrient media (below which Cu deficiency occurs) ranges from 10⁻¹⁴ to 10⁻¹⁶ M. Plants usually find a variable supply of Cu in the soil, since typically soil solution concentrations range from 10⁻⁶ to 10⁻⁹ mol.l⁻¹. Resulting amounts of calcium in our samples do not exhibit any trends. The correlation between copper and calcium for each sample position was calculated using χ -plot correlation method. Results give no significant correlation and thus it could be stated that copper accumulation does not influence calcium amount in the investigated plant compartments.

3.3. Fluorescence microscopy

In fluorescence microscopy measurements, copper-specific staining (highly specific 5-(4-dimethylaminobenzylidene)rhodanine) as well as the evaluation of autofluorescence of plant tissues were used. The advantage of autofluorescence is on the ability of some plant secondary metabolites, such as anthraquinones, coumarins, flavonoids, alkaloids, photosynthetic pigments, but especially the main components of cell walls – lignin, suberin and cutin - to emit radiation after excitation. This property was used in our study to investigate possible interactions between these compounds and copper(II) ions (changes in autofluorescence). On the other hand, presence of above mentioned compounds may misrepresent obtained results (unwanted autofluorescence). In addition, images were analyzed and the intensity of fluorescence was evaluated. As it is well-evident from the presented figure, the highest Cu concentration in dependence on used concentration was determined in the functional part of xylem (Fig. 4).

This fact is closely connected with the role of secondary xylem in water transport within plant body. Furthermore, Cu ions are able to interact with polysaccharides of the cell walls. These interactions represent the important detoxification role of cell walls, where ions of heavy metals may be compartmentalized and immobilized. This fact was confirmed not only in the case of plants, but

also in organisms with cell walls, such as algae [49,50]. Lignin represents the integral component of secondary cell walls. Its composition is based on aromatic alcohols (principally sinapyl, coniferyl and p-coumaryl), which undergo radical-based polymerization [51].

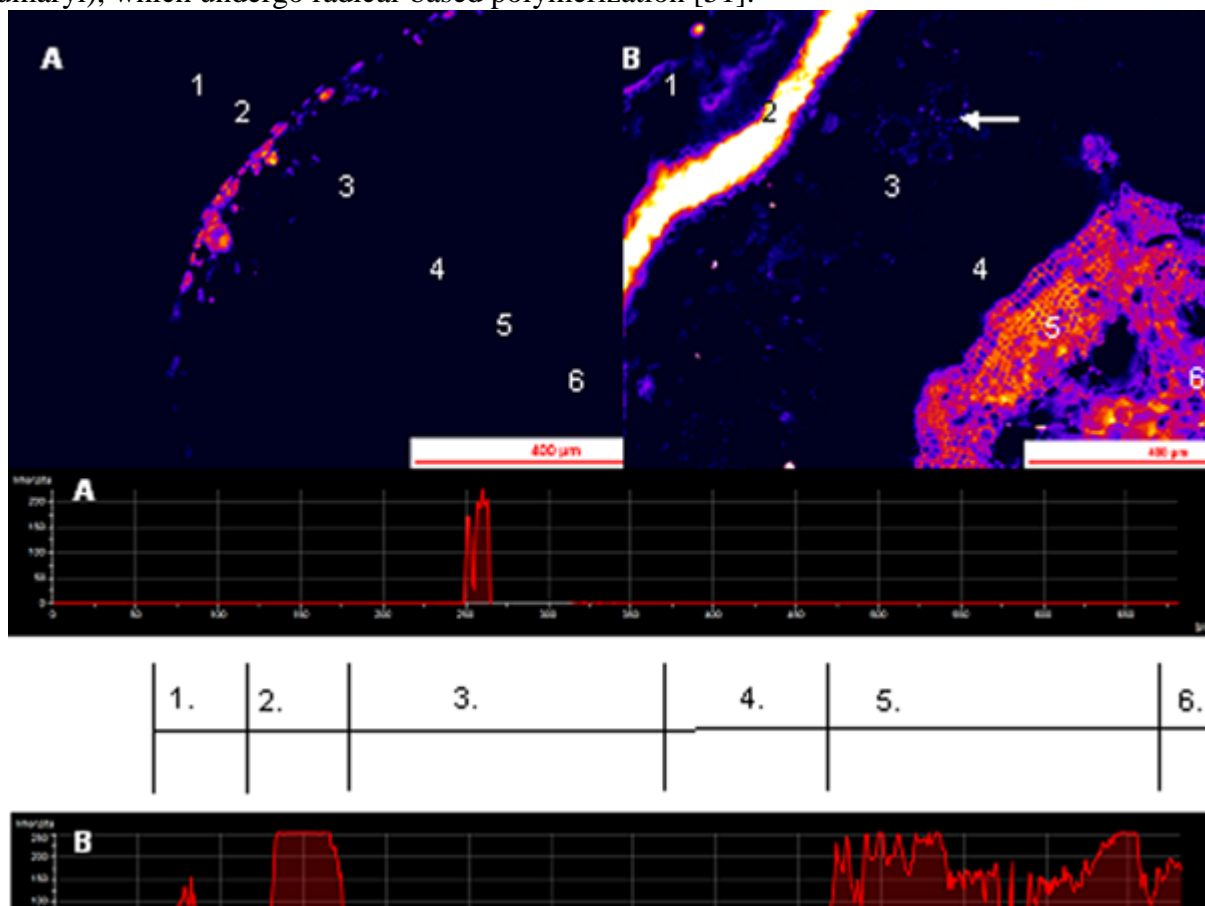


Figure 4. Distribution of Cu ions in stem tissues. 5-(4-dimethylaminobenzylidene)rhodanine staining, intensity of emission is expressed in the intensity scale. Untreated (A) and treated (B) spruce stems. Intensity of emission is shown in the form of graphs (A – untreated, B – treated): 1- the rest of dermal tissues, 2- secondary dermal tissues, 3- cortex, 4- primary and secondary phloem, 5- primary and secondary xylem, 6 – pith. White arrow indicates localization of resin duct. Note the rate of emission. Other experimental conditions see in Experimental Section.

On the other hand, lignin structure is very complicated with plenty of hydroxyl groups, which are able to interact with other compounds including heavy metals [52]. Lignin itself shows very strong autofluorescence under UV excitation [53]. This phenomenon allows determination of lignified structures as well as the rate of lignification. In our experiments we observed decrease of autofluorescence of secondary xylem compared to control. This fact is probably caused by the interactions between lignin and cell wall compounds with copper ions. Copper ions were detected also in the secondary phloem. The secondary phloem may contribute to redistribution of compounds via phloem flow. However, Cu was detected in the peripheral part of ground tissue represented by parenchyma of cortex, which is metabolically very active tissue. The localization of copper ions around secretory structures – parenchyma cells surrounding resin ducts and epithelial cells of resin ducts was well evident. However, the possibility of Cu excretion into resin ducts has to be further investigated. The above mentioned facts were useful in determining not only vertical transport of

copper ions via secondary xylem/phloem, but also transport to short distances. This transport is provided by parenchyma cells of secondary xylem/phloem, especially by radial parenchyma. In conclusion, we can propose following model of Cu transport in model stems of spruce. Copper ions are due to their solubility in water taken up and transported via secondary xylem, respectively tracheids. Chemical composition of secondary cell walls of tracheids, especially lignin, provides interactions with copper ions and their immobilization; these interactions are observable as a decrease of autofluorescence of secondary xylem. In addition, copper ions are redistributed by secondary phloem. Moreover, they are transported not only vertically, but also horizontally via xylem/phloem radial parenchyma to the ground tissue represented by cortex. For each treated sample the average intensity values of fluorescence were evaluated (total intensity of emission/total picture extent). The same values for autofluorescence measurements were evaluated. There is a visible trend where the increasing copper concentration in treatment solutions causes stronger sample fluorescence and weaker autofluorescence. Also, with increasing time of the cultivation the fluorescence strengthens and, on the other hand, the autofluorescence decays. Similar tendencies are observable also on values acquired with ICP-MS analysis. The comparison of these observations can be seen on Fig. 5. The values in all graphs (maps) were interpolated using the convolution mask.

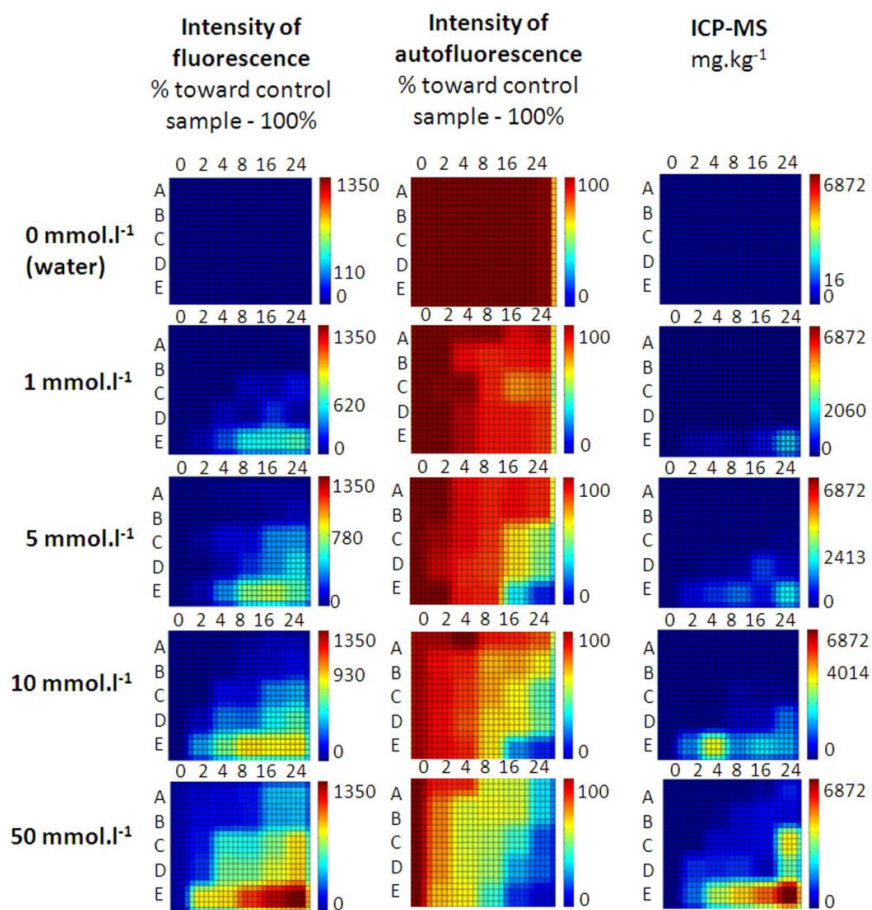


Figure 5. The comparison of fluorescence, autofluorescence and ICP-MS response in copper treated samples. Other experimental conditions see in Experimental Section.

3.4 Combination of LIBS, ICP-MS and fluorescence microscopy

LIBS data were reorganized to obtain LIBS concentration maps for spruce stem sections A to F for time intervals of 2, 4, 8, 16 and 24 hours from the beginning of the experiment and also for sections of the control sample. In total, 30 image maps were generated for each Cu concentration in the experimental solution: 0, 1, 5, 10, 50 mmol.l⁻¹. 0 mmol.l⁻¹ concentration was selected as the control for setting physiological background of images created by LIBS. This background is represented as the image noise instead of expected zero values in the locations out of the sample or the in-sample areas with zero Cu concentration. The concentration LIBS image maps were interpolated using a standard bicubic interpolation method. Thus, the images had been extended in size and smoothed what made their visual inspection easier. The maps were visualized with the application of standard jet color map for highlighting high-value concentration spots. The images were further digitally pre-processed before the following analysis. The intensity values of particular pixels were normalized based on results from ICP-MS method that provides summarized metal concentration across the whole section of the sample. The pixel value normalization overcame the main disadvantage of LIBS method – the inability to obtain absolute values of concentration for precise comparison of various samples. LIBS maps after ICP-MS normalization you can see in Fig. 6.

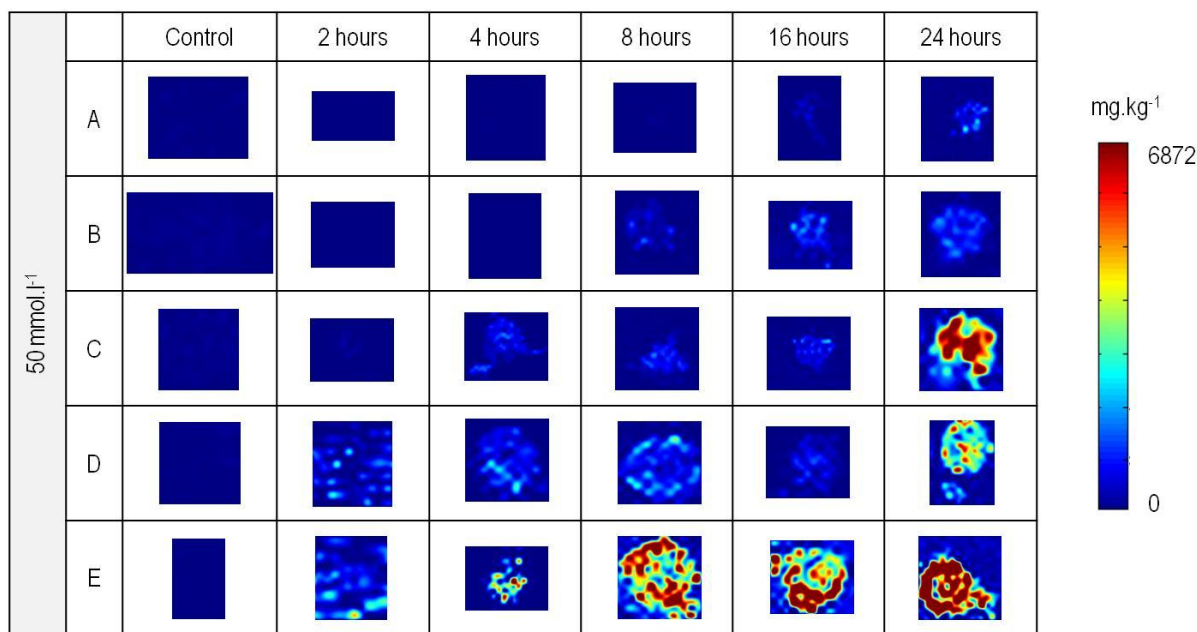


Figure 6. LIBS maps of copper distribution after ICP-MS normalization. Plant was cultivation in 50 mmol.l⁻¹ CuCl₂. Other experimental conditions see in Experimental Section.

ICP-MS results give us information about how many copper ions were at the moment transported into each position after some time of treatment. For example after 4 hours of treatment in 50 mmol.l⁻¹ copper solution were in approx. 1 mm of slice from E position 146.16 µg of copper while in A position only 0.75 µg. An exponential model, which fits in the best way, was used to express the decrease of transported copper amount with the distance from solution surface (E to A). Exponential model was also applied on the fluorescence intensity data. Resulting exponential curves from ICP-MS

and fluorescence microscopy data for 24 hours of cultivation in $50 \text{ mmol.l}^{-1} \text{ Cu}^{2+}$ solution can be seen in Fig. 7.

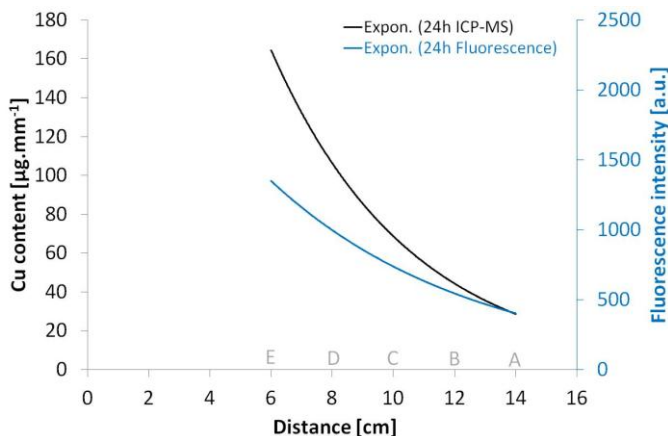


Figure 7. Exponential curves from ICP-MS and fluorescence microscopy data for 24 hours of cultivation in $50 \text{ mmol.l}^{-1} \text{ CuCl}_2$. Other experimental conditions see in Experimental Section.

Both curves are downward-sloping though the curve in the case of the fluorescence microscopy is decreasing slower. It means that at higher levels of copper amount in samples is the fluorescence response lower with comparison with ICP-MS. Thus it seems, assuming a linear calibration dependence of ICP-MS measurement, that fluorescence microscopy has in our case slightly nonlinear response and its calibration dependence is probably curved.

After that we have calculated integrals of area under the exponential curve created from ICP-MS data for specific distance intervals (see Fig. 8, $50 \text{ mmol.l}^{-1} \text{ Cu}^{2+}$ treatment for 4 hours). These results inform us about how many copper ions passed through investigated positions in total during the treatment duration. Moreover with LIBS intensity maps it is known which parts within the twig were utilized the most for copper transport. The sum of all copper signal intensities in each LIBS map corresponds to evaluated integral value and thus in maps there can be seen how much copper ions passed through specific parts on the slice or in which parts copper ions were successively accumulated, respectively. For example during 4 hours of treatment in $50 \text{ mmol.l}^{-1} \text{ CuCl}_2$ passed through E position at total $247 \mu\text{g}$ of copper ions, from that signals of $10\text{-}25 \mu\text{g}$ were observed in the area of vascular tissues (see Fig. 8). Thus it can be stated that copper ions passed through (or were accumulated in) tissues out of pith; the highest amount of copper is detectable in positions where secondary xylem and phloem is situated on the slice; indispensable amount of copper ions were also transported probably via xylem/phloem radial parenchyma to the ground tissues such cortex and secondary dermal tissues (Fig. 8). The relationship between Cu content of plants and its concentration in soil solution has linear dependence and its slope depends on plant species [8]. In our experiment we observed linear dependence between concentration of CuCl_2 solution for treatment and quantified integrals (amount of copper ions passed through investigated positions, Fig. 9).

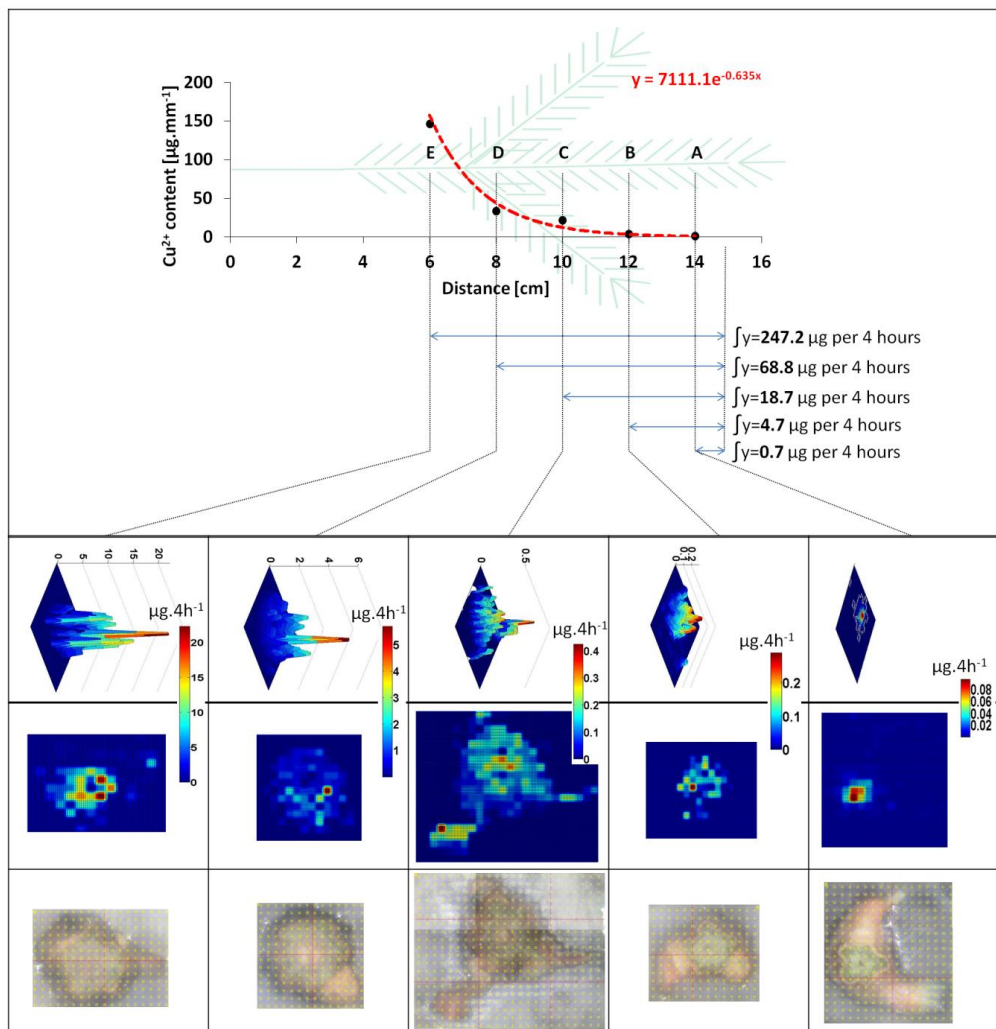


Figure 8. An application of integrals of area under the exponential curve made from ICP-MS data for specific distance intervals to LIBS intensity maps. 4 hours of cultivation in $50 \text{ mmol}\cdot\text{l}^{-1} \text{ CuCl}_2$. Other experimental conditions see in Experimental Section.

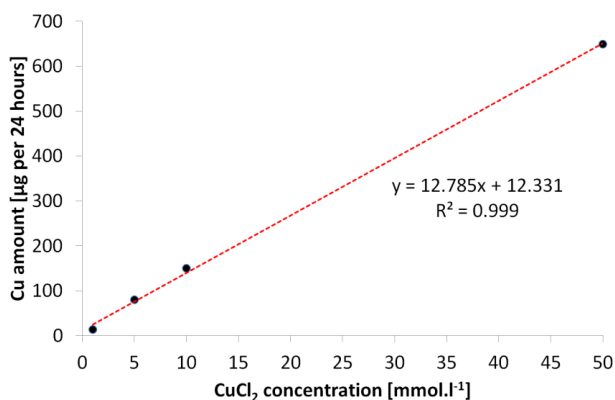


Figure 9. The relationship between CuCl_2 concentration of solution for treatment and total copper ions amount passed through E position after 24 hours. Other experimental conditions see in Experimental Section.

Similar linear tendency we have expected also in the relationship between time of cultivation and copper ions amount. Nevertheless, the uptake in time is obviously not monotonic as it is shown e.g. in Fig. 10. Similar trend was also well evident in other positions (intervals D to apex, C to apex, B to apex and A to apex). It seems that after some time the uptake of copper ions is for a while stopped and continues again later. These results indicate the possibility of three different uptake processes, from which the first involves natural plant metal uptake, the second is connected to the plant protecting mechanisms and the third one is a simple diffusion after the plant metabolism collapse.

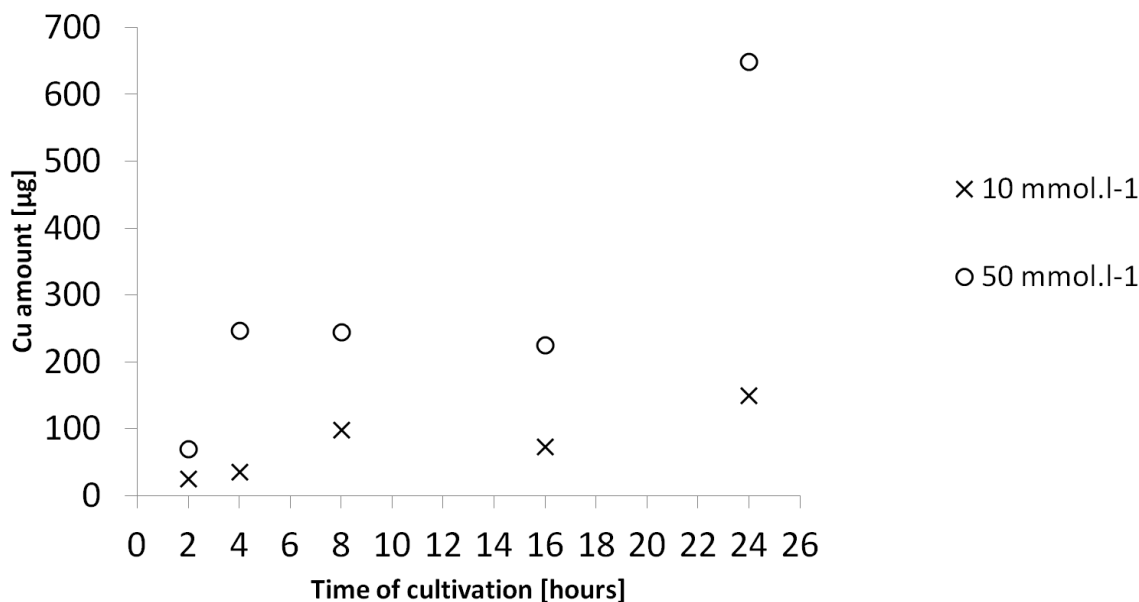


Figure 10. The relationship between time of cultivation and total copper ions amount passed through E position for different CuCl_2 concentration of solution for cultivation. Other experimental conditions see in Experimental Section.

4. CONCLUSIONS

Copper spatial distributions in the slices of annual terminal stem parts of *Picea abies* (L.) Karsten cultivated in Cu^{2+} solutions were observed with double-pulse LIBS experimental approach in orthogonal reheating mode. The ICP-MS solution analysis was used in order to obtain the quantitative information for LIBS data normalization. While LIBS allows the spatial distribution observation, ICP-MS analysis gives just the quantitative information with no spatial distribution. Fluorescence microscopy is useful to obtain information connected to spatial distribution, but does not provide the quantitative information. Thus fluorescence pictures were used for the comparison with LIBS distribution maps and the fluorescence intensity (or the increase in autofluorescence) was used for the comparison with ICP-MS quantitative results. The correlation of results from these three methods gives the final conclusion about quantitative and spatial distribution of elements within samples. In control samples there are very low contents of Cu in comparison with treated samples and the changes of concentrations are minimal. In 1 mmol.l^{-1} treated samples there are the strongest concentrations noticeable after long time duration (16 and 24 hours) and also in places near the solution surface (D,

E). With further increase of the solution concentration, Cu^{2+} spreads also to more distant positions in shorter time and so the concentration gradient seems to be still steeper. In our experiment Cu amount was often much higher than the phytotoxic values, especially in E position close to the solution surface. There is no significant correlation between copper and calcium amounts. The amount of copper transported into investigated positions (A-E) has an exponential trend for each time of the treatment, which is visible from both ICP-MS and fluorescence data. Both exponential curves are downward-sloping. The curve of the fluorescence microscopy is decreasing slower. It means that at higher levels of copper amount in samples there is the fluorescence response lower with comparison with ICP-MS one. Thus it seems, assuming a linear calibration dependence of the ICP-MS measurement, that the fluorescence microscopy has slightly nonlinear response and its calibration curve is probably little bit curved. Results show that copper ions passed through (or were accumulated in) tissues out of the pith; the highest amount of copper is detectable in positions where secondary xylem and phloem is situated on the slice; indispensable amount of copper ions were also transported probably via xylem/phloem radial parenchyma to the ground tissues such cortex and secondary dermal tissues. Linear dependence between the concentration of CuCl_2 solution for treatment and the amount of transported copper ions was observed, whereas not monotonic relationship between the cultivation interval and the amount of copper ions was detected. These results indicate the possibility of three different uptake processes, from which the first involves natural plant metal uptake, the second is connected to the plant protecting mechanisms and the third one is simple diffusion after the plant metabolism collapse.

ACKNOWLEDGEMENTS

We acknowledge the support by the project “CEITEC - Central European Institute of Technology” (CZ.1.05/1.1.00/02.0068) from European Regional Development Fund. This work was also supported by grants ME09015 and ME10061 of the Ministry of Education, Youth and Sports of the Czech Republic and by “Specific research” FSI-S-10-56, and FSI-S-11-22 of Brno University of Technology. Research at Oak Ridge National Laboratory was supported by the US Department of Energy (DOE), Office of Science, Biological and Environmental Research program through the Consortium for Carbon Sequestration in Terrestrial Ecosystems. Oak Ridge National Laboratory is managed by UT-Battelle, LLC, for the DOE under Contract DEAC05-00OR22725. We would like to acknowledge the help of K. Procházková in preparation of the manuscript.

References

1. J. R. Peralta-Videa, M. L. Lopez, M. Narayan, G. Saupé and J. Gardea-Torresdey, *Int. J. Biochem. Cell Biol.*, 41 (2009) 1665.
2. E. D. Schulze, E. Beck and K. Müller-Hohenstein, *Plant Ecology*, Springer-Verlag, Berlin, 2005.
3. I. Yruela, *Braz. J. Plant Physiol.*, 17 (2005) 145.
4. B. Halliwell and J. M. C. Gutteridge, *Biochem. J.*, 219 (1984) 1.
5. S. Clemens, *Planta*, 212 (2001) 475.
6. J. L. Hall and L. E. Williams, *J. Exp. Bot.*, 54 (2003) 2601.
7. W. Maksymiec, *Photosynthetica*, 34 (1997) 321.
8. A. Kabata-Pendias and H. Pendias, *Trace Elements in Soils and Plants*, CRC Press, Florida, 1992.

9. I. D. Pulford and C. Watson, *Environ. Int.*, 29 (2003) 529.
10. C. Maurice and A. Lagerkvist, *J. Soil Contam.*, 9 (2000) 31.
11. I. D. Pulford, C. Watson and S. D. McGregor, *Environ. Geochem. Health*, 23 (2001) 307.
12. W. Rosselli, C. Keller and K. Boschi, *Plant Soil*, 256 (2003) 265.
13. R. Metzner, H. U. Schneider, U. Breuer and W. H. Schroeder, *Plant Physiol.*, 147 (2008) 1774.
14. J. S. Becker, R. C. Dietrich, A. Matusch, D. Pozebon and V. L. Dressier, *Spectroc. Acta Pt. B-Atom. Spectr.*, 63 (2008) 1248.
15. J. S. Becker, M. Zoriy, B. Wu and A. Matusch, *J. Anal. At. Spectrom.*, 23 (2008) 1275.
16. M. Galiova, J. Kaiser, K. Novotny, O. Samek, L. Reale, R. Malina, K. Palenikova, M. Liska, V. Cudek, V. Kanicky, V. Otruba, A. Poma and A. Tucci, *Spectroc. Acta Pt. B-Atom. Spectr.*, 62 (2007) 1597.
17. J. Kaiser, K. Novotny, M. Z. Martin, A. Hrdlicka, R. Malina, M. Hartl, V. Adam and R. Kizek, *Surf. Sci. Rep.*, 67 (2012) 233.
18. M. M. Burrell, C. J. Earnshaw and M. R. Clench, *J. Exp. Bot.*, 58 (2007) 757.
19. P. Porizka, D. Prochazka, Z. Pilat, L. Krajcarova, J. Kaiser, R. Malina, J. Novotny, P. Zemanek, J. Jezek, M. Sery, S. Bernatova, V. Krzyzanek, K. Dobranska, K. Novotny, M. Trtilek and O. Samek, *Spectroc. Acta Pt. B-Atom. Spectr.*, 74-75 (2012) 169.
20. Q. Sun, M. Tran, B. W. Smith and J. D. Winefordner, *Can. J. Anal. Sci. Spectrosc.*, 44 (1999) 164.
21. O. Samek, J. Lambert, R. Hergenroder, M. Liska, J. Kaiser, K. Novotny and S. Kukhlevsky, *Laser Phys. Lett.*, 3 (2006) 21.
22. J. Kaiser, O. Samek, L. Reale, M. Liska, R. Malina, A. Ritucci, A. Poma, A. Tucci, F. Flora, A. Lai, L. Mancini, G. Tromba, F. Zanini, A. Faenov, T. Pikuz and G. Cinque, *Microsc. Res. Tech.*, 70 (2007) 147.
23. J. Kaiser, M. Galiova, K. Novotny, R. Cervenka, L. Reale, J. Novotny, M. Liska, O. Samek, V. Kanicky, A. Hrdlicka, K. Stejskal, V. Adam and R. Kizek, *Spectroc. Acta Pt. B-Atom. Spectr.*, 64 (2009) 67.
24. M. Galiova, J. Kaiser, K. Novotny, J. Novotny, T. Vaculovic, M. Liska, R. Malina, K. Stejskal, V. Adam and R. Kizek, *Appl. Phys. A-Mater. Sci. Process.*, 93 (2008) 917.
25. V. Juve, R. Portelli, M. Boueri, M. Baudelet and J. Yu, *Spectroc. Acta Pt. B-Atom. Spectr.*, 63 (2008) 1047.
26. L. C. Trevizan, D. Santos, R. E. Samad, N. D. Vieira, C. S. Nomura, L. C. Nunes, I. A. Rufini and F. J. Krug, *Spectroc. Acta Pt. B-Atom. Spectr.*, 63 (2008) 1151.
27. L. C. Trevizan, D. Santos, R. E. Samad, N. D. Vieira, L. C. Nunes, I. A. Rufini and F. J. Krug, *Spectroc. Acta Pt. B-Atom. Spectr.*, 64 (2009) 369.
28. M. Z. Martin, N. Labbe, N. Andre, R. Harris, M. Ebinger, S. D. Wullschleger and A. A. Vass, *Spectroc. Acta Pt. B-Atom. Spectr.*, 62 (2007) 1426.
29. M. Z. Martin, A. J. Stewart, K. D. Gwinn and J. C. Waller, *Appl. Optics*, 49 (2010) C161.
30. E. P. Colangelo and M. L. Guerinot, *Curr. Opin. Plant Biol.*, 9 (2006) 322.
31. W. H. O. Ernst, J. A. C. Verkleij and H. Schat, *Acta Bot. Neerl.*, 41 (1992) 229.
32. R. M. Welch, *Crit. Rev. Plant Sci.*, 14 (1995) 49.
33. D. Hynek, L. Krejcova, J. Sochor, N. Cernei, J. Kynicky, V. Adam, L. Trnkova, J. Hubalek, R. Vrba and R. Kizek, *Int. J. Electrochem. Sci.*, 7 (2012) 1802.
34. D. Hynek, J. Prasek, J. Pikula, V. Adam, P. Hajkova, L. Krejcova, L. Trnkova, J. Sochor, M. Pohanka, J. Hubalek, M. Beklova, R. Vrba and R. Kizek, *Int. J. Electrochem. Sci.*, 6 (2011) 5980.
35. A. Kleckerova, P. Sobrova, O. Krystofova, J. Sochor, O. Zitka, P. Babula, V. Adam, H. Docekalova and R. Kizek, *Int. J. Electrochem. Sci.*, 6 (2011) 6011.
36. O. Krystofova, O. Zitka, S. Krizkova, D. Hynek, V. Shestivska, V. Adam, J. Hubalek, M. Mackova, T. Macek, J. Zehnalek, P. Babula, L. Havel and R. Kizek, *Int. J. Electrochem. Sci.*, 7 (2012) 886.

37. P. Majzlik, A. Strasky, V. Adam, M. Nemeč, L. Trnkova, J. Zehnalek, J. Hubalek, I. Provazník and R. Kizek, *Int. J. Electrochem. Sci.*, 6 (2011) 2171.
38. J. Sochor, O. Zitka, D. Hynek, E. Jilkova, L. Krejčova, L. Trnkova, V. Adam, J. Hubalek, J. Kynický, R. Vrba and R. Kizek, *Sensors*, 11 (2011) 10638.
39. S. Clemens, M. G. Palmgren and U. Kramer, *Trends Plant Sci.*, 7 (2002) 309.
40. V. Supalkova, D. Huska, V. Diopan, P. Hanustiak, O. Zitka, K. Stejskal, J. Baloun, J. Pikula, L. Havel, J. Zehnalek, V. Adam, L. Trnkova, M. Beklova and R. Kizek, *Sensors*, 7 (2007) 932.
41. V. Supalkova, J. Petrek, J. Baloun, V. Adam, K. Bartusek, L. Trnkova, M. Beklova, V. Diopan, L. Havel and R. Kizek, *Sensors*, 7 (2007) 743.
42. P. Babula, V. Adam, R. Opatrilova, J. Zehnalek, L. Havel and R. Kizek, *Environ. Chem. Lett.*, 6 (2008) 189.
43. O. Zitka, O. Krystofova, P. Sobrova, V. Adam, J. Zehnalek, M. Beklova and R. Kizek, *J. Hazard. Mater.*, 192 (2011) 794.
44. O. Zitka, M. A. Merlos Rodrigo, V. Adam, N. Ferrol, M. Pohanka, J. Hubalek, J. Zehnalek, L. Trnkova and R. Kizek, *J. Hazard. Mater.*, 203-204 (2012) 257.
45. O. Zitka, H. Skutkova, O. Krystofova, P. Sobrova, V. Adam, J. Zehnalek, L. Havel, M. Beklova, J. Hubalek, I. Provazník and R. Kizek, *Int. J. Electrochem. Sci.*, 6 (2011) 1367.
46. D. Potesil, J. Petrlova, V. Adam, J. Vacek, B. Klejdus, J. Zehnalek, L. Trnkova, L. Havel and R. Kizek, *J. Chromatogr. A*, 1084 (2005) 134.
47. V. Diopan, K. Stejskal, M. Galiova, V. Adam, J. Kaiser, A. Horna, K. Novotny, M. Liska, L. Havel, J. Zehnalek and R. Kizek, *Electroanalysis*, 22 (2010) 1248.
48. U. Krämer and S. Clemens, *Functions and homeostasis of zinc, copper, and nickel in plants*, Springer, Berlin, 2006.
49. I. Michalak and K. Chojnacka, *Eng. Life Sci.*, 10 (2010) 209.
50. M. Senden, F. J. M. Vanpaassen, A. Vandermeer and H. T. Wolterbeek, *Plant Cell Environ.*, 15 (1992) 71.
51. V. Chiang, *In Vitro Cell. Dev. Biol.-Anim.*, 47 (2011) S28.
52. M. Torre, A. R. Rodriguez and F. Sauracalixto, *J. Agric. Food Chem.*, 40 (1992) 1762.
53. V. De Micco and G. Aronne, *Biotech. Histochem.*, 82 (2007) 209.